1521-0103/377/3/407–416$35.00
THE JOURNAL OF PHARMACOLOGY AND EXPERIMENTAL THERAPEUTICS

https://doi.org/10.1124/jpet.120.000438
J Pharmacol Exp Ther 377:407–416, June 2021

Development of CVN424: A Selective and Novel GPR6 Inverse Agonist Effective in Models of Parkinson Disease[S]

Nicola L. Brice, Hans H. Schiffer, Holger Monenschein, Victoria J. Mulligan, Keith Page, Justin Powell, Xiao Xu, Toni Cheung, J. Russell Burley, Huikai Sun, Louise Dickson, Sean T. Murphy, Nidhi Kaushal, Steve Sheardown, Jason Lawrence, Yun Chen, Darian Bartkowski, Anne Kanta, Joseph Russo, Natalie Hosea, Lee A. Dawson, Stephen H. Hitchcock, and Mark B. Carlton

Cerevance Ltd, Cambridge, United Kingdom (N.L.B., V.J.M., K.P., J.P., X.X., T.C., J.R.B., L.D., S.S., J.L., L.A.D., M.B.C.); and Takeda California, San Diego, California (H.H.S., H.M., H.S., S.T.M., N.K., Y.C., D.B., A.K., J.R., N.H., S.H.H.)

Received November 26, 2020; accepted March 29, 2021

ABSTRACT

GPR6 is an orphan G-protein–coupled receptor that has enriched expression in the striatopallidal, indirect pathway and medium spiny neurons of the striatum. This pathway is greatly impacted by the loss of the nigro-striatal dopaminergic neurons in Parkinson disease, and modulating this neurocircuitry can be therapeutically beneficial. In this study, we describe the in vitro and in vivo pharmacological characterization of (R)-1-(2-(4-(2,4-difluorophenoxy)piperidin-1-yl)-3-((tetrahydrofuran-3-yl)amino)-7,8-dihydropyrido[3,4-b]
pyrazin-6(5H)-yl)ethan-1-one (CVN424), a highly potent and selective small-molecule inverse agonist for GPR6 that is currently undergoing clinical evaluation. CVN424 is brain-penetrant and shows dose-dependent receptor occupancy that attained brain 50% of receptor occupancy at plasma concentrations of 6.0 and 7.4 ng/ml in mice and rats, respectively. Oral administration of CVN424 dose-dependently increases locomotor activity and reverses haloperidol-induced catalepsy. Furthermore, CVN424 restored mobility in bilateral 6-hydroxydopamine lesion model of Parkinson disease. The presence and localization of GPR6 in medium spiny neurons of striatum postmortem samples from both nondemented control and patients with Parkinson disease were confirmed at the level of both RNA (using Nuclear Enriched Transcript Sort sequencing) and protein. This body of work demonstrates that CVN424 is a potent, orally active, and brain-penetrant GPR6 inverse agonist that is effective in preclinical models and is a potential therapeutic for improving motor function in patients with Parkinson disease.

SIGNIFICANCE STATEMENT

CVN424 represents a nondopaminergic novel drug for potential use in patients with Parkinson disease.

Introduction

Parkinson disease (PD) is currently the second-most-common neurodegenerative disorder and has the fastest growth in incidence rate (Dorsey and Bloem, 2018). Loss of the dopamine-producing cells in the substantia nigra and resultant striatal dopamine signaling dysregulation are neuropathological hallmarks of PD that drive motor symptoms (Bellucci et al., 2016).

The dopamine D1 and D2 receptor–expressing medium spiny neurons (MSNs) of the direct and indirect pathways, respectively, are morphologically indistinguishable but functionally distinct (Lenz and Lobo, 2013). They form two opposing circuits: the direct (striatonigral) pathway, which initiates motor activity, and the indirect (striatopallidal) pathway, which suppresses or terminates motor activity (Freeze et al., 2013). The progressive loss of the dopaminergic neurons of the substantia nigra pars compacta in PD results in a decline in striatal dopamine, leading to neuronal hypoactivity in the direct pathway and hyperactivity in the indirect pathway (Kravitz et al., 2010). This imbalance in the output pathways of the striatum is thought to underlie the motor symptoms of PD, such as tremors and bradykinesia (Ryan et al., 2018).

Replacing this dopaminergic loss remains the mainstay of PD treatment, with patients being typically treated

Financial support for this work was provided by Cerevance Ltd. and Takeda Pharmaceuticals. All authors are employees of Cerevance Ltd. or Takeda Pharmaceuticals.
https://doi.org/10.1124/jpet.120.000438.
[S] This article has supplemental material available at jpet.aspetjournals.org.

ABBREVIATIONS: CB1, cannabinoid receptor 1; CNS, central nervous system; CVN424, (R)-1-(2-(4-(2,4-difluorophenoxy)piperidin-1-yl)-3-((tetrahydrofuran-3-yl)amino)-7,8-dihydropyrido[3,4-b]pyrazin-6(5H)-yl)ethan-1-one; DAT, dopamine transporter; DBS, deep brain stimulation; DRD1, dopamine D1 receptor; DRD2, dopamine D2 receptor; DTT, dithiothreitol; GFAP, glial fibrillary acidic protein; GPCR, G-protein–coupled receptor; GPR, G-protein–coupled receptor member; Ki, equilibrium dissociation constant; LC/MS/MS, liquid chromatography with tandem mass spectrometry; MSN, medium spiny neuron; NETSseq, Nuclear Enriched Transcript Sort sequencing; OFA, open field arena; 6-OHDA, 6-hydroxydopamine; PD, Parkinson disease; p.o., per os(oral); RO, receptor occupancy; RO_{50}, 50% of receptor occupancy.

with L-DOPA, the precursor of dopamine (Salat and Tolosa, 2013). Although patients initially experience some symptomatic benefit, a gradual loss of efficacy tends to limit its long-term effectiveness, and many patients develop troublesome adverse effects, such as L-DOPA–induced dyskinesias (Brooks, 2008; Chen, 2011; Hauser et al., 2018; You et al., 2018). Although other therapies, including dopamine receptor agonists, have been developed, these agents tend to be less effective and primarily useful early in the disease or as adjunctive L-DOPA therapy (de Bie et al., 2020; Poewe and Mahlknecht, 2020).

Nondopaminergic therapies for the motor symptoms of Parkinson disease may have the potential to delay, replace, or reduce the dose of L-DOPA required to treat the disease and therefore decrease the onset of significant dopamine-related side effects (Müller, 2017; Nutt and Bohnen, 2018).

The indirect pathway projects into the globus pallidus, which in turn innervates the subthalamic nucleus. Over the past decade, it has been demonstrated that deep brain stimulation (DBS) of these output nuclei, particularly the subthalamic nucleus, provides significant and often dramatic motor improvement for PD patients (Whitmer et al., 2012; Mansouri et al., 2018). DBS is highly effective but because of its invasive nature and associated risks, including mortality and high costs of neurosurgery, is reserved for a small subset of patients that meet strict criteria (Pollak, 2013). Nonetheless, the efficacy of DBS demonstrates that selectively targeting the indirect pathway may be sufficient to control motor symptoms of PD. Thus, a drug that pharmacologically suppresses activity in the indirect pathway with minimal effect on the direct pathway could attenuate the Parkinsonian motor symptoms without the troublesome adverse effects commonly elicited by non–pathway selective drugs.

G-protein–coupled receptor member (GPR) 6 is a GPCR that is highly expressed in indirect pathway neurons relative to direct pathway neurons and has little expression detected in other regions of the CNS or peripheral tissues (Lobo et al., 2007; Heiman et al., 2008). GPR6 is still classified as an orphan receptor, although some efficacy has been seen with potential endogenous ligands, including endocannabinoids and sphingosine-1-phosphate (Uhlenbrock et al., 2002; Ignatov et al., 2003; Laun and Song, 2017; Shrader and Song, 2020). The receptor is Gαs-coupled with high constitutive activity, which increases cAMP and thereby continuously activates the indirect striatopallidal pathways (Ignatov et al., 2003; Tanaka et al., 2007). Attenuation of GPR6-induced activity could, therefore, reduce the pathologic hyperactivity seen within the indirect pathway in PD.

Here we describe the development and pharmacological evaluation of a novel, potent, and selective small-molecule inverse GPR6 agonist, (R)-1-(2-(4-(2,4-difluorophenoxy)piperidin-1-yl)-3-((tetrahydrofuran-3-yl)amino)-7,8-dihydropyrido[3,4-b]pyrazin-6(5H)-yl)ethan-1-one (CVN424). CVN424 shows excellent cross-species brain penetration and striatal GPR6 receptor occupancy. In vivo, CVN424 attenuates haloperidol-induced catalepsy and locomotor behavior and reverses 6-hydroxydopamine (6-OHDA) lesion-induced locomotor deficits. We also show the expression of GPR6 mRNA and protein present in both nondemented control and PD donor striatal postmortem human tissue.

Materials and Methods

Compounds and Reagents

CVN424 was synthesized by Takeda, and RL-338 was synthesized by Envoy Therapeutics, Inc., FL (Fig. 1). For binding studies, RL-338 was radiolabeled with three tritium atoms by Quotient Bioresearch (Cardiff, UK). For in vivo dosing, CVN424 was formulated in 0.5% methylcellulose (Sigma Chemical Co., Poole, UK) except for the receptor occupancy and 6-OHDA study in which CVN424 was formulated in 20% Captisol (CYDEX Pharmaceuticals Inc). Haloperidol (Sigma Chemical Co.) was prepared in saline. All reagents were from Sigma unless otherwise stated.

Cell Culture

T-REx-CHO cells stably expressing human GPR6, GPR3, or GPR12 driven by a doxycycline-inducible promoter of the pcDNA5/TO Vector (Invitrogen) were cultured in F12K medium (Gibco; Life Technologies) containing 10% tetracycline free FBS (HyClone; Fisher Scientific), 1% penicillin/streptomycin, and 200 μg/ml hygromycin B. Receptor expression was induced with the addition of 2 μg/ml doxycycline to cell culture medium for 12 hours. CHO-K1 cells (American Type Culture Collection) transiently transfected with mammalian expression plasmids for human, rat, or mouse GPR6 were also grown in F12K medium containing 10% FBS and 1% penicillin/streptomycin.

In Vitro Characterization of CVN424

Membrane Binding. The binding characteristics of CVN424 were assessed using a competition radioligand binding assay with a filtration-based format developed featuring membranes prepared from T-REx-CHO-GPR6 cells. The total concentration of protein in the membrane preparations was determined using the biochemical bicinchoninic acid assay (Thermo Fisher). In vitro pharmacological profiling showed that RL-338 is a potent and highly selective GPR6 inverse agonist inhibiting GPR6 cAMP signaling in time-resolved fluorescence energy transfer assays with an EC_{50} = 16 nM and >100-fold selectivity against GPR3 and GPR12 . ^{3}H-RL-338 demonstrated high affinity for human GPR6 receptors stably expressed in T-REx-CHO cells (Kd = 2.4 or 5 nM dependent on synthesized radioligand batch) in saturation binding assays. Similar Kd values were obtained for ^{3}H-RL-338 binding to membranes from human, mouse, and rat GPR6 transiently expressed in CHO-K1 cells: mouse Kd = 5.7 nM, rat Kd = 8.1 nM, and human Kd = 7.3 nM.

Mouse GPR6 expression plasmid in pCMV6 backbone was obtained from Origene (USA) reference number MC212312. Rat GPR6 cDNA was custom-synthesized based on rat genome and inserted in expression vector pJX607. Plasmid for expression of human GPR6 was in pcDNA3.1 backbone obtained from Missouri S&T cDNA resource (GPR0060000). CHO-K1 cells were transient-transfected with species-specific GPR6 expression plasmids using Xtreme Gene 9 transfection reagent (Roche) according to the manufacturer protocol. Membranes were prepared 48 hours after transfection.

To determine CVN424 binding affinity to GPR6 containing membrane preparations, assay-ready 96-well plates (Greiner) containing serial dilutions of CVN424 were prepared (1 μl/well) in DMSO, to which assay buffer [50 mM Tris (pH 7.4), 50 mM NaCl, 6 mM $MgCl_2$,

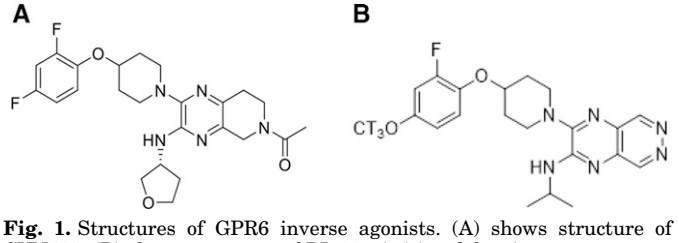

Fig. 1. Structures of GPR6 inverse agonists. (A) shows structure of CVN424. (B) shows structure of RL-338 (tritiated form).

fatty acid–free 0.1% bovine serum albumin, proteinase inhibitor cocktail] was added (39 μl/well), and the plates were mixed for 10 minutes on a plate shaker. Next, 40 μl per well of radioligand ^{3}H-RL-338 (specific activity 85 Ci/mmol) prepared in assay buffer was added (final assay concentration 5.0 nM). CVN424 concentrations tested ranged from 5 μM (top concentration) to 0.06 nM (lowest concentration) with 1:5 dilution steps. Binding reactions were initiated by adding 40 μl of total membranes obtained from cells expressing human GPR6 receptors. Membranes were prepared in assay buffer and added at 15 μg/well, mixed, and incubated for 2 hours at room temperature. Reactions were filtered through filtermates (1450-421, Filtermate A; Perkin Elmer) and washed five times with 50 mM Tris (pH 7.4), 50 mM NaCl, 6 mM $MgCl_2$, and fatty acid–free 0.1% bovine serum albumin using a Tomtec Harvester 96 instrument. Filters were dried in the microwave, and scintillator sheet (1450-411; PerkinElmer) was melted onto them and heat-sealed before counts per minute per well were quantified in Microbeta Trilux instrument (Perkin Elmer). Before use, filtermates were presoaked in 0.5% polyethylenimine solution for 3 hours with gentle shaking, which was followed by air drying overnight. The same protocol was used for saturation binding assays to determine radioligand ^{3}H-RL-338 affinity to GPR6. Different concentrations of radioligand RL-338 ranging from 32 (high concentration) to 0.015 nM (low concentration) with 1:2 dilution steps were tested to generate saturation curves and obtain the equilibrium dissociation constant Kd. Nonspecific background binding of ^{3}H-RL-338 was determined using 10 μM of an unlabeled structurally diverse potent and selective GPR6 inverse agonists (unpublished data). IC_{50} and Kd values were calculated using nonlinear regression analysis in Prism (GraphPad). Saturation curves were fitted using Prism non-linear regression (One site-Total) equation and non-specific binding without constraints. Dose-response curves were fitted to the four-parameter variable slope model without constrains in Prism to obtain IC_{50}s. Ki values were calculated using the Cheng-Prusoff equation (Cheng and Prusoff, 1973). CVN424 fully displaced ^{3}H-RL-338 from GPR6 and displayed binding properties that were consistent with a single binding site.

Functional Activity Assessment. Functional activity of the inverse agonist CVN424 to reduce apparent constitutive activity across species was measured in a Perkin Elmer's LANCE HTRF cAMP assay with CHO-K1 cells transiently transfected with the mammalian expression plasmids carrying mouse or rat GPR6 cDNAs. These constructs were transfected using Xtreme Gene 9 transfection reagent (Roche). Briefly, 150,000 CHO-K1 cells were plated in 10-cm dishes and incubated overnight at 37°C with 5% CO_2. The next day, 30 μl of Xtreme Gene 9 was added to 1.5 ml Opti-MEM media (Life Technologies), and this was followed by adding 10 μg DNA, which was then incubated at room temperature for 25 minutes. Mixture was added to cells, and this was followed by 20–24 hours incubation at 37°C with 5% CO_2. Cells were replated into 96-well black plates (Corning) and returned overnight to the incubator to allow the cells to adhere.

Selectivity of CVN424 for human GPR6 in comparison with human GPR3 and GPR12 was evaluated in functional HTRF cAMP assays with T-REx-CHO cells (Invitrogen) stably expressing human GPR6, GPR3, or GPR12.

To measure cAMP modulation cells were replated into 96-well black plates (Corning) and returned overnight to the incubator to allow the cells to adhere. For stable GPR6, GPR3, or GPR12 cell lines, receptor expression was induced with the addition of 2 μg/ml doxycycline to cell culture medium for 12 hours. A 10 mM stock solution of CVN424 was prepared in DMSO. Serial dilutions of CVN424 were prepared with Kreb's Ringer buffer (plus 0.5% fatty acid–free bovine serum albumin and 300 μM IBMX), added to the plates (20 μl/well), and incubated for 45 minutes at 37°C. Final CVN424 concentrations tested ranged from 30 μM (top concentration) to 0.5 nM (lowest concentration) with 1:3 dilution steps. Next, Eu-labeled cAMP tracer (10 μl) diluted in cAMP detection/lysis buffer with 10 μl ULight-anti-cAMP diluted in the same buffer was added to the cells. Plates were incubated for 60 minutes at room temperature, and then time-resolved fluorescence energy transfer was measured on an EnVision plate reader (Perkin Elmer). CVN424 displayed full inverse agonism efficacy (Maximal effect (Emax) 100%) at GPR6, GPR3, and GPR12, completely inhibiting observed apparent constitutive activity windows in the respective CHO-K1–based receptor expression systems. IC_{50} values were calculated by fitting data to the four-parameter variable slope model without constrains using nonlinear regression analysis in Prism (GraphPad).

To determine the selectivity of CVN424 at 1 and 10 μM, a CEREP screen against 110 receptors, ion channels, transporters, and enzymes was conducted at Eurofins (www.eurofinsdiscoveryservices.com) using their standard assay protocols.

Animals

Mice and rats were housed in accordance with institutional standards. They were maintained on a 12-hour light/dark cycle and had access ab libitum to food and water. Experiments performed in Europe were conducted in accordance with the European Communities directive 2010/63/EU. Experiments conducted in the United States were in accordance with the Guide for the Care and Use of Laboratory Animals (National Research Council, 2011). Animal research in India was performed according to the guidance from the Committee for the Purpose of Control and Supervision of Experiments on Animals. All experiments were in accordance with and approved by the Institutions' Animal Care and Use Committees. Male rodents were used across the behavior and receptor occupancy studies. Female rats were used for the 6-OHDA model, as there is extensive prior validation with female rats due to their reduced sensitivity to stress that can significantly decrease activity in male rats (Faraday, 2002). Cross-sex pharmacokinetic evaluation was conducted to ensure parity of compound exposure in these studies (unpublished data).

Receptor Occupancy

Dose-dependent receptor occupancy (RO) by CVN424 on striatal GPR6 was determined using a label-free in vivo liquid chromatography with tandem mass spectrometry (LC/MS/MS)-based RO method in male mice and rats (n = 4/dose/species) using RL-338 (vehicle: 10% DMSO, 0.5% Tween 80, 89.5% PBS) as a tracer.

Male C57BL/6J mice (30 ± 10 g; Suven, India) or Sprague-Dawley rats (250 ± 50 g; Vivo Biotech Ltd, Hyderabad, India) (n = 4/dose/species) were first administered vehicle or CVN424 at 1.0, 3.0, 5.0, 10, and 30 mg/kg, p.o. At 60 minutes postdose, animals were administered the nontritiated form of RL-338 at 100 (mice) or 30 μg/kg (rats) i.v. After 30 (mice) or 45 minutes (rats) post–RL-338 dose, animals were euthanized, and trunk blood was collected into tubes containing sodium heparin. Plasma was separated by centrifugation (1900g, 4°C for 10 minutes). Brains were removed, frozen on dry ice, and stored below −50°C until being processed further for RL-338 extraction.

Brain and plasma samples from all animals were analyzed for CVN424 levels by LC/MS/MS (API4000 MDS; SciEx). Briefly, samples were thawed on ice. Acetonitrile was added to each sample at a volume (microlitre) of four times the weight (milligram) of tissue. Samples were homogenized (7 to 8 W power using sonic probe dismembrator; Fisher Scientific) and centrifuged for 10 minutes at 12,000g, and the supernatant solution was subjected to quantification of RL-338 using LC/MS/MS.

For plasma samples for each 50 μl of sample, 200 μl of acetonitrile containing 0.1% formic acid was added. Samples were vortex-mixed, which was followed by centrifugation at 21,000g for 20 minutes; the supernatant solutions were assayed for quantification of CVN424 using LC/MS/MS.

GPR6 receptor occupancy of CVN424 was calculated based on the ratio method: % receptor occupancy = $100*\{1-[\text{ratio}_t-1]/(\text{ratio}_v)]\}$. Ratio_t = ratio of RL-338 concentrations measured in striata (GPR6-specific brain region) to RL-338 concentrations measured in cerebellum (brain region without detectable GPR6 expression) in individual animals pretreated with CVN424. Ratio_v = average ratio of RL-338 concentrations measured in striata to RL-338 concentrations

measured in cerebellum for the vehicle-pretreated group. Plasma 50% of receptor occupancy (RO_{50}) values were calculated in Prism (GraphPad) by fitting % RO values and correlating plasma exposures of CVN424 (nanogram per milliliter) to the four-parameter variable slope model in nonlinear regression analysis.

Behavioral Studies

Locomotor activity was measured in an open field arena (OFA) (Med-Associates). Male C57BL/6J mice (11 to 12 weeks; Jackson Laboratories, ME) were acclimatized to the equipment for 1 hour before being administered CVN424 (0.1, 0.3, 1, or 3 mg/kg; p.o.; n = 12–15) or vehicle (0.5% methylcellulose). Immediately after dosing, the mice were placed back into their respective chambers, and the distance traveled in the arena was measured for 1 hour. Locomotor activity was quantified as the disruptions in three 16 infrared photo beam arrays that circumscribed each enclosure. Immediately after the behavior experiment, plasma samples were taken from each animal. The total plasma EC_{50} to modulate locomotor activity was calculated in Prism (GraphPad) by fitting total distance traveled values and correlating plasma exposures of CVN424 (nanogram per milliliter) to the four-parameter variable slope model in nonlinear regression analysis.

For haloperidol-induced catalepsy experiments, male C57BL/6J mice (11 to 12 weeks; Jackson Laboratories) were acclimated to the procedure room for 1 to 2 hours. During this period, mice carried out training/acclimatization to the bar test (Med Associates, MED-PCIV) by placing them in the bar test chambers for 2 minutes, and this was followed by four to five practice bar test runs.

Following acclimatization, mice were dosed orally with CVN424 (0.1 (n = 11), 0.3 (n = 9), 1 (n = 9), or 3 mg/kg (n = 11); p.o.) or vehicle (0.5% methylcellulose; p.o.; n = 8). Immediately after oral dosing, haloperidol (0.45 mg/kg, i.p.) was administered to all mice except for a separate saline (intraperitoneal) control group (n = 6). Thirty minutes post-treatment, animals were tested for catalepsy for 2 minutes by placing their forepaws on a 5 cm–high bar, and the time spent immobile in that position was measured using an automated scoring instrumentation.

On completion of behavioral testing (locomotor activity and catalepsy), mice were culled, brains were removed, and terminal blood samples were collected into tubes containing K_2EDTA. The plasma was separated by centrifugation, and the brains were removed onto ice and homogenized. Plasma and brain homogenate samples were extracted using a protein precipitation extraction method, and LC/MS/MS was performed on an MDS Sciex API5500 mass spectrometer (AB SCIEX, Concord, ON, Canada) equipped with a Shimadzu liquid chromatography system and an LEAP autosampler. A reverse-phase gradient method running at a flow rate of 0.6 ml/min on a Phenomenex Kinetex C18 5.0 100A column (2.1 mm i.d. × 50 mm) (Phenomenex, Inc., Torrance, CA) was used for analyte separation.

The mobile phases used were water (A) and acetonitrile (B), and both were supplemented with formic acid (0.04%, v/v). The gradient program used the following liquid chromatography parameters for mobile phase B: 10 (%v/v) during period 0.2–1.5 minutes, 95 (%v/v) during period 1.5–1.9 minutes, and 10 (%v/v) during period 1.9–2.5 minutes.

CVN424 was ionized under a positive ion spray mode and detected through the multiple-reaction monitoring of a mass transition pair at a mass-to-charge ratio of 474.241/289.200. Calibration curves of CVN424 were established using standards, and the peak area ratios of the analyte against an internal standard were used to quantify samples.

6-OHDA Lesion Model

Prior to surgery, locomotor activity of 20 female Sprague Dawley rats (269 to 300 g, Charles River) was assessed in the OFA for 3 hours (prelesion) to determine baseline activity.

On the day of surgery but 30 minutes prior to surgery, the rats were administered pargyline (5 mg/kg; i.p.) and desipramine (10 mg/kg; i.p.) to optimize subsequent 6-OHDA availability and to increase specificity for toxicity to dopaminergic neurons. Under anesthesia with isoflurane, rats were placed in a Kopf small animal stereotaxic apparatus, and 6-OHDA (20 μg in 3 μl; 0.5 μl/min) was injected into the striatum at coordinates Anterior-Posterior: (medial-lateral : dorsal-ventral, 1, ±3, −5 mm relative to bregma (Paxinos and Watson, 2007). Animals were allowed to recover from the surgery for 28 days before behavioral testing.

To determine the success of the lesion, locomotor activity of all animals was assessed in the OFA (Linton Instrumentation, UK) for 3 hours to determine the postlesion behavioral deficit compared with the presurgery recording.

On the day of compound testing, animals were placed in the OFA for 30 minutes for habituation and then were administered vehicle (p.o.; n = 6) or CVN424 at 5 mg/kg or 10 mg/kg (p.o.; n = 7 per group) and returned to the OFA for 2 hours recording of locomotor activity.

Immediately after the completion of the behavioral assessment, DAT binding was performed to determine extent of lesion. Animals received an overdose of pentobarbital (intraperitoneal) and were transcardially perfused with ice-cold 0.9% saline containing 0.2% heparin. Brains were removed and immediately frozen.

The levels of striatal DAT were assessed by [^{125}I]-RTI-121–binding autoradiography in cryostat-cut 20-μm sections. Thawed slides were placed in PBS for 30 minutes at room temperature. Sections were incubated in PBS containing 10 pM [^{125}I]-RTI-121 (specific activity 2200 Ci/μmol; Perkin-Elmer) for 90 minutes at room temperature. Slides were washed (2 × 20 minutes) in PBS at 4°C, rinsed in ice-cold distilled water, and air-dried. Densitometric analysis of autoradiograms of three striatal sections per animal were analyzed using MCID software (Image Research Inc, ON, Canada) and compared with brains from nonlesioned rats.

Statistical Analyses

For behavioral analysis in the 6-OHDA locomotor activity, the haloperidol catalepsy models, and locomotor activity studies, data were analyzed with a one-way ANOVA with Dunnett's post hoc using InVivoStat (v.3.4) comparing CVN424-dosed groups to vehicle.

For the 6-OHDA model data from the DAT binding and prelesion to postlesion comparisons, statistical analyses were performed using an unpaired t test (Graphpad Prism v.6.03).

Human Tissue Experiments

Human tissue samples were obtained from the Miami Brain Bank (University of Miami). All human tissues used in this study were collected from donors for whom a full written consent was obtained for use of material and clinical information in accordance with the Declaration of Helsinki. Data and material were managed in compliance with the UK Human Tissue Act. Clinical records confirmed donors with Parkinson disease were diagnosed during life [n = 5 (three female and two male)]. Control donors [n = 9 (five male and four female)] had not been diagnosed with a CNS-related disorder and died from a non–CNS-related cause. The average age of the PD donors was 70.4 years with a post-mortem delay of 13.3 hours. The average age for the control donors was 63.4 years with a post-mortem delay of 12.6 hours. All donors were Caucasian.

Nuclear Enriched Transcript Sort Sequencing

Protocols for nuclei isolation from tissue samples are essentially as described in Kriaucionis and Heintz (2009) and Xu et al. (2018). Briefly, human putamen samples were homogenized in medium [0.25 M sucrose, 150 mM KCl, 5 mM $MgCl_2$, 20 mM Tricine pH 7.8, 0.15 mM spermine, 0.5 mM spermidine, 1 mM dithiothreitol (DTT), 20 U/ml Superase-In RNase inhibitor, 40 U/ml RNasin ribonuclease inhibitor, mini EDTA-free protease inhibitor cocktail] that was supplemented

with 50% iodixanol solution (50% iodixanol/Optiprep, 150 mM KCl, 5 mM $MgCl_2$, 20 mM Tricine pH 7.8, 0.15 mM spermine, 0.5 mM spermidine, mini EDTA-free protease inhibitor cocktail, 1 mM DTT, 20 U/ml Superase-In RNase inhibitor, 40 U/ml RNasin ribonuclease inhibitor) posthomogenization and laid on a 27% iodixanol cushion. Nuclei were pelleted by centrifugation for 25 minutes at 10,000*g* at 4°C (Eppendorf 5427 R centrifuge, FA-45-12-17 rotor).

After nuclei isolation, resuspended nuclei were fixed with 1% formaldehyde for 8 minutes at room temperature and then quenched with 0.125 M glycine for 5 minutes. Nuclei were pelleted at 1000*g* for 4 minutes at 4°C and then washed once with homogenization medium and once with Wash Buffer (PBS, 0.05% Triton X-100, 50 ng/ml bovine serum albumin, 1 mM DTT, 10 U/μl Superase-In RNase inhibitor). Nuclei were resuspended in 100 μl PrimeFlow RNA Wash Buffer (00-19180; Invitrogen) and labeled with PrimeFlow Target Probes (Invitrogen) [DARPP32/PPP1R1B (Alexa Fluor A647), dopamine D1 receptor (DRD1) (Alexa Fluor A568), and dopamine D2 receptor (DRD2) (Alexa Fluor A488); samples were centrifuged at 1000*g* for 3 minutes at 21°C.

Prior to flow cytometry, nuclei were costained with 4′,6-diamidino-2-phenylindole to 0.01 mg/ml final concentration. Nuclei were analyzed and sorted using BD FACSAria fusion (BD Biosciences, San Jose, CA) flow cytometer using the 355-, 488-, 561-, and 640-nm lasers. All samples were first gated using forward and side scatter gates to exclude debris followed by a single nuclei 4′,6-diamidino-2-phenylindole gate to exclude aggregated nuclei. Analysis was performed using FACSDiva (BD) or FlowJo software. To reduce RNA degradation, all nuclei samples were sorted at 4°C and stored at −80°C before being processed for RNA extraction. RNA was converted to sequencing libraries using the Tecan Trio kit and quantitated using a Nanodrop, and the size range was confirmed by Agilent Bioanalyser. Libraries were combined into equimolar pools of 32 and sequenced on an Illumina NextSEq. Five hundred (high output) in 75 bp paired end mode.

To assess RNA-sequencing quality control, alignment, and quantitation, FastQC (http://www.bioinformatics.babraham.ac.uk/projects/fastqc/) was used for initial quality control. Adapter trimming was performed with Cutadapt v1.12 (Martin, 2011). Reads were aligned to the hg38 human genome build (National Center for Biotechnology Information primary analysis set) using STAR aligner v2.5.2b (Dobin et al., 2013) with splice junction files generated from Gencode release 27 and RefSeq GRCh38.p10. Postalignment quality control was performed by examination of the STAR alignment metrics, Picard tools v2.8.2 (CollectRNASeqMetrics) (https://broadinstitute.github.io/picard/), and RSeQC v2.6.4 (tin.py) (Wang et al., 2012). Expression quantitation was performed with htseq-count v0.6.1p1 (Anders et al., 2015) using a custom annotation file based on RefSeq in which both exonic and intronic reads are counted for each gene. Differential gene expression differences were calculated using DESeq (Robles et al., 2012).

GPR6 Histology

Formalin-fixed, paraffin-embedded blocks of caudate-putamen from three nondemented control donors were used to investigate human GPR6 expression. Sections were cut from these blocks, at a thickness of 5 μm on a rotary microtome (RM2255; 535 blades; Leica). Sections were mounted on microscope slides (Fisher Scientific).

An Agilent Dako PT Link (PT200) was used for dewaxing of tissue sections and antigen retrieval, using high-pH antigen retrieval buffer [EnV FLEX TRS, high pH (50×); K800421-2; Agilent Dako]. Briefly, slides were inserted into the PT Link, where they were prewarmed to 65°C, brought up to 97°C for 20 minutes, and then cooled to 65°C. Slides were then bathed in wash buffer (K802321-2 EnVision FLEX Mini Kit, High pH; Agilent Dako) at room temperature for a minimum of 5 minutes.

A rabbit polyclonal GPR6 antibody was custom-generated with epitopes against the extracellular domain of human GPR6. In short, a fusion protein consisting of the extracellular domain of human GPR6 fused to the Ig-Fc tag was expressed in *Escherichia coli*, affinity-purified, and injected into rabbits to generate a polyclonal antibody recognizing human and rodent GPR6 receptors (unpublished data). This antibody was applied to the relevant tissue sections (1:500 dilution; Takeda, CA). A rabbit polyclonal anti–glial fibrillary acidic protein (GFAP) antibody (1:5000 dilution; ab7260, lot GR3202608-1; Abcam) was included as a positive assay control, and a rabbit isotype-specific immunoglobulin (1.2 μg/ml; X090302-2; Agilent Dako) was used as a negative assay control.

The staining process used the Agilent Autostainer Link 48 and an EnVision FLEX Mini Kit (K802321-2; Agilent Dako). Briefly, sections were rinsed in wash buffer, and then FLEX peroxidase was applied for 5 minutes and rinsed again in wash buffer before application of primary antibody or IgG control. Labeling of the primary antibody with FLEX/horseradish peroxidase and 3,3-diaminobenzidine system was followed by counterstaining with FLEX hematoxylin (K800821-2; Agilent Dako). Sections were then rinsed in deionized water and wash buffer before being dehydrated through a rising ethanol gradient (50%, 70%, 95%, absolute ethanol × 2; 4 minutes each; room temperature; Fisher Chemical). Excess ethanol was shaken off before slides were placed in a xylene bath (PRC/R/201; Pioneer Research Chemicals) twice to clear (4 minutes; room temperature). Slides were coverslipped with DPX mountant (6522; Sigma) and glass coverslips (12373128 Fisherbrand Borosilicate Glass Coverslips). Sections were analyzed using an Axioskop 2 plus microscope (Zeiss).

Results

CVN424 was discovered through a directed medicinal chemistry campaign after a high-throughput screen targeting human GPR6 coupled via a β-arrestin assay system. The structure is shown in Fig. 1A.

CVN424 Is a Potent and Selective Inverse Agonist for GPR6. Binding affinity of CVN424 for GPR6 was determined using CHO-K1 cell membranes expressing GPR6 in a competitive radioligand binding assay with tritiated RL-338 (Fig. 1B), a second potent GPR6 inverse agonist with an EC_{50} of 16 nM in the cAMP assay. Cell membranes from CHO-K1 cells stably expressing human GPR6 and CVN424 demonstrated a Ki of 9.4 nM ($n = 9$). To compare the binding affinity of CVN424 across species, membranes were prepared from CHO-K1 cells transiently transfected with cDNA from mouse or rat GPR6. CVN424 demonstrated similar binding affinities (within 2-fold) across species (Table 1).

To determine the functional activity and selectivity of CVN424, CHO-K1 cells were stably transfected with GPR6, GPR3, or GPR12. CVN424 completely blocked GPR6-induced cAMP levels with an EC_{50} ± S.D. of 55.1 ± 24.8 nM ($n = 76$), demonstrating its activity as a potent and fully efficacious GPR6 inverse agonist (Fig. 2A). In contrast, in the GPR3- and GPR12-expressing cell lines, CVN424 was less potent but still fully efficacious in reducing cAMP levels with an EC_{50} ± S.D. of 1921 ± 859 nM ($n = 18$) and 6965 ± 3189 nM ($n = 18$), respectively (Fig. 2, B and C). This equates to a functional selectivity of CVN424 for GPR6 over GPR3 of 35-fold and GPR6 over GPR12 of 126-fold.

Further selectivity of CVN424 was tested in a CEREP panel of 110 radioligand binding and enzyme assays (CEREP SA; Eurofins, Celle-Levescault, France). Of these 110 assays, CVN424 modulated activity ≥50% in just four defined receptor assays at 10 μM (Table 2) with an $IC_{50} > 1$ μM.

CVN424 Achieves High Levels of GPR6 Occupancy in Brain. To understand target engagement, brain penetration, and plasma concentrations required for CVN424 to

TABLE 1
Cross-species in vitro binding affinity of CVN424 against GPR6
Radioligand binding assays were performed with total cell membranes isolated from CHO-K1 cells stably expressing human GPR6 or from CHO-K1 cells transiently transfected with mammalian expression plasmids carrying rat or mouse GPR6 cDNAs.

Stable Expression of Human GPR6 Ki ± S.D.	Transient Expression of Rodent GPR6	
	Rat Ki ± S.D.	Mouse Ki ± S.D.
9.4 ± 8.2 nM (n = 9)	3.0 ± 1.3 nM (n = 3)	1.6 ± 0.6 nM (n = 3)

TABLE 2
Selectivity of CVN424: Percent inhibition of receptors by CVN424 at 1 and 10 μM
Summary of results from the CEREP selectivity screen in which CVN424 was assayed against 110 receptors and enzymes at two concentrations. Results shown are the assays in which CVN424 showed >50% inhibition at 10 μM plus the inhibition of CVN424 against the CB1 receptor at 1 and 10 μM.

Target	% Inhibition	
	1 μM	10 μM
Adrenergic α1A (rat)	21	54
Adrenergic α1B (rat)	6	50
Adrenergic α1D (human)	16	71
Sigma, nonselective (guinea pig)	17	55
Cannabinoid CB1 (human)	14	34

achieve GPR6 RO in the striatum, a label-free in vivo LC/MS/MS-based RO method was developed using a nontritiated form of RL-338 (Fig. 1B) as a cold tracer in both rats and mice. In mice, the mean ± S.D. GPR6 RO of CVN424 measured in the striatum at 0.3, 1.0, 3.0, 10, and 30 mg/kg p.o. was 48.6% ± 24.0%, 69.2% ± 7.8%, 92.7% ± 2.3%, 97.1% ± 2.3%, and 99.7% ± 2.0%, respectively. The calculated dose for 50% occupancy (ED_{50}) was 0.34 mg/kg, and the total plasma concentration at RO_{50} in striatum was 6.0 ng/ml (Fig. 3A). However, in rats, the mean ± S.D. striatal GPR6 receptor occupancy obtained at 5.0, 10, and 30 mg/kg p.o. was 30.76 ± 24.6, 72.16 ± 14.3, and 98.16 ± 2.6, respectively. The calculated occupancy ED_{50} was 7.25 mg/kg, and its total plasma RO_{50} was 7.4 ng/ml (Fig. 3B). See also Supplemental Tables 1 and 2

CVN424 Induces Locomotor Activity in Mice. Activation of the indirect pathway of the striatum limits locomotor activity in mice (Jenkins et al., 1980). Thus, it was hypothesized that CVN424 would reduce activity of the indirect pathway via inverse agonism of GPR6 and thereby increase locomotor activity. Mice were administered vehicle or CVN424 at 0.1, 0.3, 1, or 3 mg/kg (n = 12–15 per group), and locomotor activity was measured. CVN424 dose-dependently increased locomotor activity ($P < 0.0001$; $F = 13.48$ one-way ANOVA) with Dunnett's post hoc analysis at 0.3 mg/kg ($P = 0.0015$), 1 mg/kg ($P = 0.0034$), and 3 mg/kg ($P < 0.0001$) (Fig. 4A). To confirm exposure, terminal blood and brain samples were taken for pharmacokinetic analysis at the end of the locomotor experiment. CVN424 showed a dose-dependent increase in plasma and brain concentration with an average brain-to-plasma ratio of 0.4. The total plasma EC_{50} to modulate locomotor activity was 12 ng/ml.

CVN424 Reverses Haloperidol-Induced Catalepsy in Mice. The ability for CVN424 to reverse haloperidol-induced catalepsy was tested at 0.1, 0.3, 1, and 3 mg/kg p.o. CVN424 dose-dependently attenuated haloperidol-induced catalepsy at 30 minutes post-treatment. One-way ANOVA confirmed an effect of the treatment ($P < 0.0001$; F 15.47) with Dunnett's post hoc analysis confirming the effect of CVN424 at 0.1 ($P = 0.0002$) and 0.3, 1, and 3 mg/kg (all $P < 0.0001$) (Fig. 4B). A satellite group of animals was dosed simultaneously for the purposes of pharmacokinetic analysis for plasma and brain. The EC_{50} of CVN424 to reduce catalepsy was determined to be 4.4 ng/ml total plasma concentration.

CVN424 Improves Locomotor Function in Bilateral 6-OHDA Lesioned Rats. To determine whether CVN424 has anti-Parkinsonian activity, the compound was tested as a monotherapy in a rat bilateral 6-OHDA lesion model of Parkinson disease. The primary outcome measure was locomotor performance in the OFA. 6-OHDA lesion caused a decrease of 44% in locomotor activity recorded over a 3-hour period (Supplemental Fig. 1A), and depletion of dopamine terminals was confirmed by dopamine transporter staining after completion of study (Supplemental Fig. 1C). CVN424 was assessed in this model at 5 and 10 mg/kg. At 10 mg/kg, CVN424 reversed the motoric deficits induced by 6-OHDA compared with vehicle-dosed animals increasing locomotor activity by 164% ($P = 0.0097$; $F = 6.17$ one-way ANOVA; $P = 0.005$; Dunnett's post hoc analysis) (Fig. 5).

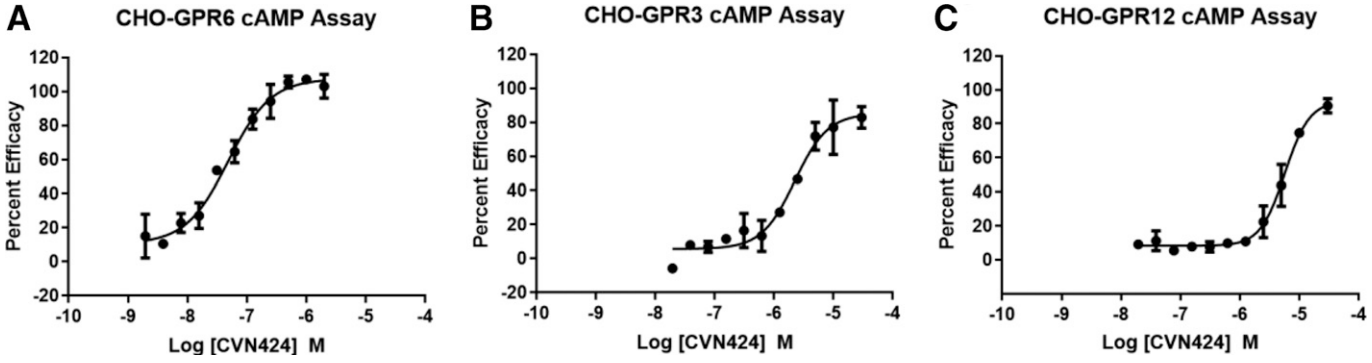

Fig. 2. CHO-K1 cells stably transfected with human GPR6 (A), GPR3 (B), or GPR12 (C) treated with CVN424 for 45 minutes and assayed for cAMP levels. Results represent examples from independent repeat experiments. Data in each graph displayed as mean ± S.D. of technical replicates. The EC_{50} ± S.D. for CVN424 to inhibit GPR6 activity in cAMP assays was determined to be 55.1 ± 24.8 nM (n = 76), in contrast to EC_{50} ± S.D. of 1927 ± 859 nM (n = 18) and 6965 ± 3189 nM (n = 18) for GPR3 and GPR12, respectively. CVN424 displayed full inverse agonism efficacy (Maximal effect (Emax) around 100%) at GPR6, GPR3, and GPR13, completely inhibiting the observed apparent constitutive activity windows in the respective CHO-K1–based receptor expression systems.

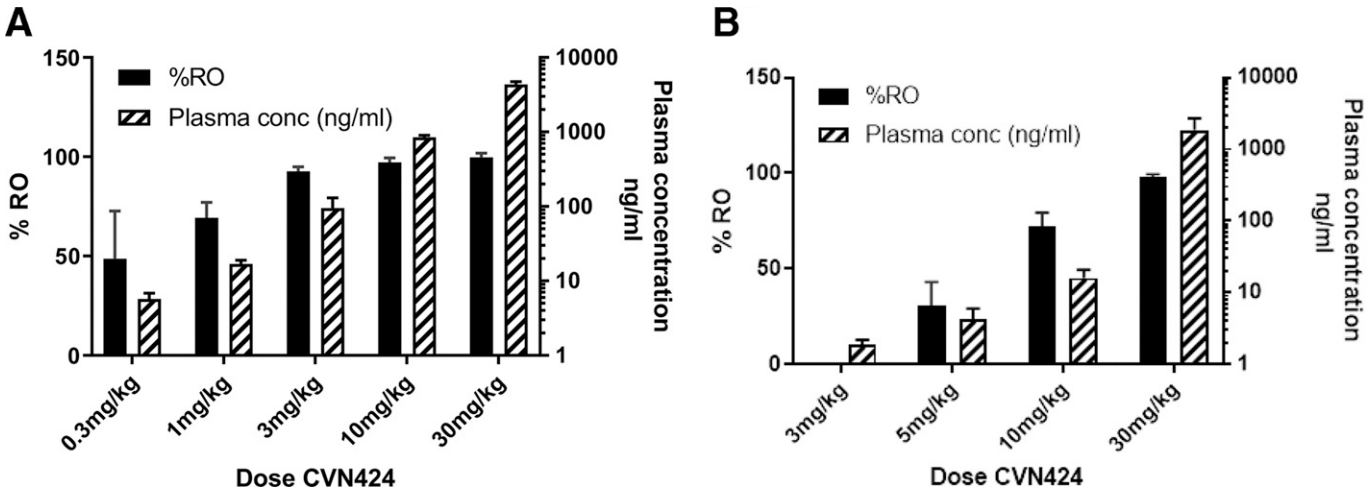

Fig. 3. Receptor occupancy of CVN424 in the striatum (mean ± S.D., $n = 4$ per data point). (A) Receptor occupancy and plasma exposures of CVN424 in male C57BL/6J mice pretreated (60 minutes) orally with CVN424 followed by RL-338 administration (100 μg/kg, i.v.), and mice were sacrificed after 30 minutes. Calculated ED_{50} was 0.34 mg/kg, and corresponding plasma RO_{50} was 6.0 ng/ml after 90 minutes. (B) Receptor occupancy and plasma exposures of CVN424 in male Sprague Dawley rats pretreated (60 minutes) orally with CVN424 followed by RL-338 (30 μg/kg, i.v.), and rats were sacrificed after 30 minutes. Calculated ED_{50} was 7.25 mg/kg, and corresponding plasma RO_{50} was 7.4 ng/ml after 105 minutes.

GPR6 Expression Is Not Changed in Indirect MSNs from Patients with PD and Non-PD Controls. We used Nuclear Enriched Transcript Sort sequencing (NETSseq), a method of measuring expression from specific cell types from human post-mortem tissue (Xu et al., 2018) to determine the expression levels of GPR6 in direct and indirect MSNs from control and donors with PD. To demonstrate the selectivity of this technique, we also show the relative expression of mRNA for the dopamine receptors DRD1 and DRD2, which show the expected preference for direct and indirect MSNs, respectively (Fig. 6). We confirmed that similar to what we observed in rodents, GPR6 is highly expressed in D2-receptor–expressing indirect MSNs. D1-receptor–expressing MSNs have approximately 20-fold–lower levels of GPR6 mRNA expression than D2-expressing MSNs (DESeq; Student's t test $P = 3.9e^{-07}$). It is important to confirm the presence of potential drug targets in the target population, especially in a progressively degenerating disease, such as Parkinson disease. Therefore, we compared the expression of GPR6 in D2-receptor–expressing indirect MSNs from the putamen of both control donors ($n = 18$) and donors diagnosed with Parkinson disease ($n = 12$). We observed no difference in GPR6 mRNA levels between control and donors with Parkinson disease ($P = 0.85$).

GRP6 Protein Is Expressed in a Subpopulation of MSNs in the Striatum. To confirm that the GPR6 RNA detected by NETSseq in MSNs is translated into proteins, we conducted immunohistochemistry on human post-mortem caudate putamen from control donors ($n = 3$) using an anti-GPR6

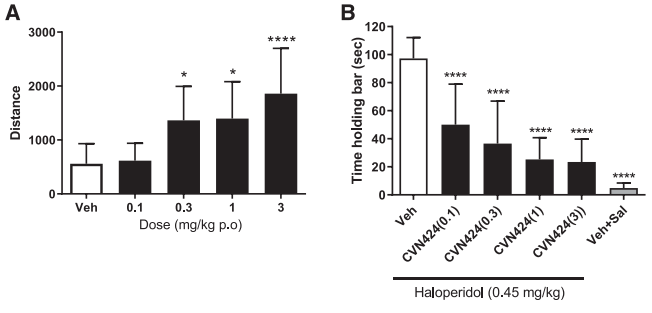

Fig. 4. (A) Effect of CVN424 on locomotor activity. Male C57Bl/6J mice were administered vehicle (0.5% methylcellulose) (white bar) or CVN424 at 0.1, 0.3, 1, and 3 mg/kg (p.o.) (black bars), and locomotor distance (centimeter) was recorded for the next 1 hour. Results indicate that CVN424 increased locomotor activity compared with vehicle control. Data represented as mean ± S.D.; $*P < 0.05$; $****P < 0.0001$ vs. vehicle control. (B) Haloperidol was dosed at 0.45 mg/kg to induce catalepsy. CVN424 dose-dependently reduced the haloperidol-induced catalepsy compared with vehicle (white bar). ANOVA $F = 15.47$; $P < 0.0001$ Dunnett's post hoc analysis $****P < 0.0001$. Gray barrepresents the data from animals treated with saline and vehicle (0.5% methylcellulose). All data are presented as mean ± S.D. .

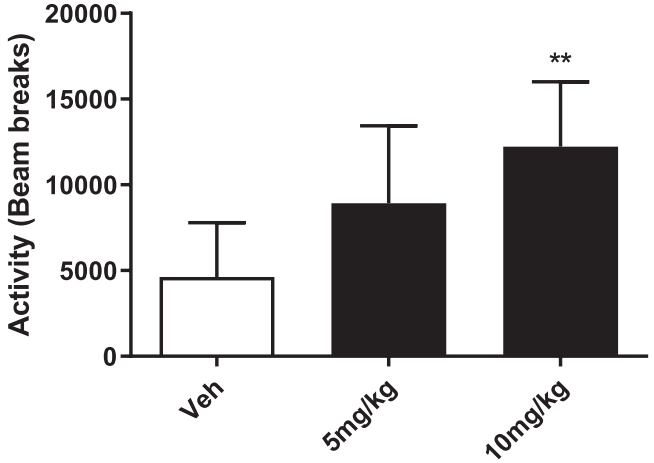

Fig. 5. CVN424 dose-dependently reverses locomotor deficits in the bilateral 6-OHDA model of Parkinson disease. Rats were treated with 6-OHDA to induce motor deficits and then dosed with vehicle (white bar) or CVN424 (black bars) p.o. and locomotor activity in an OFA measured. Data are presented as mean ± S.D. (ANOVA $F = 6.17$; $P = 0.0097$, Dunnett's post hoc analysis $**P < 0.01$). veh, vehicle.

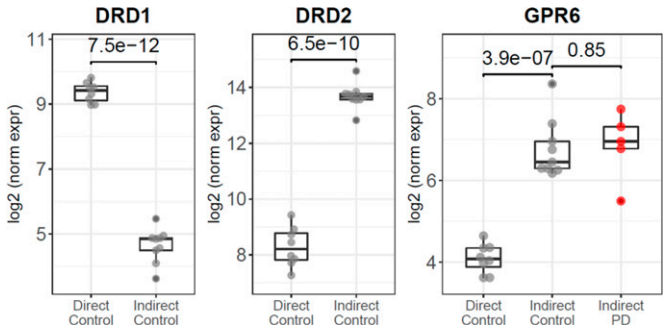

Fig. 6. NETSseq data from human post-mortem samples showing expression in MSNs from the putamen. Log2 expression of DRD1, DRD2, and GPR6 in either direct or indirect MSNs from control donors (gray dots) or donors diagnosed with Parkinson disease (red dots). Statistical analysis by Student's *t* test (values shown).

antibody. We confirmed selective localization of GPR6 expression to a subpopulation of MSNs (Fig. 7A) in line with the NETSseq RNA observations. Positive and negative controls yielded the expected results (Fig. 7, B and C).

Discussion

GPR6 has enriched expression in the indirect pathway MSNs of the striatum in rodents and has been postulated as a potential pharmacological target for treating Parkinson disease (Oeckl et al., 2014; Oeckl and Ferger, 2016). In this study, we describe the development and pharmacological characterization of a first-in-class small-molecule GPR6 inverse agonist, CVN424, and its in vivo evaluation in preclinical models relevant to Parkinson disease. In addition, we demonstrate the highly specific expression of GPR6 RNA and protein in subpopulations of striatal neurons from healthy and Parkinson disease post-mortem tissue.

We show that CVN424 has high binding affinity for GPR6 with a comparable affinity across species homologs from human, rat, and mouse, thus confirming the relevance and use of these species in the assessment of CVN424's pharmacology. Functionally, CVN424 reduced cAMP levels in human GPR6-expressing CHO-K1 cells, demonstrating its activity as an inverse agonist. The functional potency of CVN424 was lower than its binding affinity (55 nM vs. 17 nM, respectively). These differences between potency and affinity are not unexpected, especially as different cell systems were used (Strange, 2008). Selectivity of CVN424 for GPR6 was compared with its most homologous family members, GPR3 and GPR12, and against a broad panel of receptors, channels, and enzymes. CVN424 was at least 100-fold selective against all targets evaluated with the exception of GPR3, which was 35-fold. However, we expect this level of selectivity to give sufficient confidence that at therapeutic doses, CVN424 is mediating its effects via GPR6. For example, in rat 6-OHDA study10 mg/kg reversed the motor deficits and this dose in the RO study produced a total plasma concentration of 16.1 ng/ml (30 nM). Since the EC_{50} for GPR3 is 1927 ± 859 nM, it is unlikely that functional inhibition of GPR3 is attained at these exposure concentrations.

Included in the crossreactivity screen was the human CB1 receptor to which CVN424 showed very low binding affinity (34% at 10 μM). Although GPR6 is still classed as an orphan GPCR, there have been reports proposing candidate ligands, including the previously reported CB2 receptor antagonist SR144528 (0.62 μM) (Laun et al., 2018) and endocannabinoids, including endocannabinoid-like *N*-acrylamides, such as *N*-arachidonoyl dopamine (Uhlenbrock et al., 2002; Laun and Song, 2017; Breivogel et al., 2018; Shrader and Song, 2020). The latter is described as an endogenous inverse agonist and is detected in the striatum (Ji et al., 2014), although it is not thought to be specific for GPR6 (Grabiec and Dehghani, 2017). The endocannabinoid-like *N*-acrylamides have recently been shown to modulate GPR6 in an in vitro *β*-arrestin assay, a recombinant assay system that is independent of G-protein coupling. There was no effect of these ligands on a GPR6-mediated G-protein–dependent cAMP accumulation assay (Shrader and Song, 2020). Evidence from the 6-OHDA–lesion model suggests that the absence of dopaminergic signaling to the striatum results in increases in cAMP levels, which is linked to Parkinsonian-like motor deficits (Giorgi et al., 2011). Here we clearly demonstrate that CVN424 functionally inhibits cAMP in recombinant GPR6-expressing CHO-K1 cells. Furthermore, GPR6−/− mice have been shown to have a 20% decrease in striatal cAMP levels when compared with wild-type littermates (Oeckl et al., 2014). Thus, we can speculate that CVN424 is reducing striatal cAMP levels in vivo, and it is this that is mediating the observed

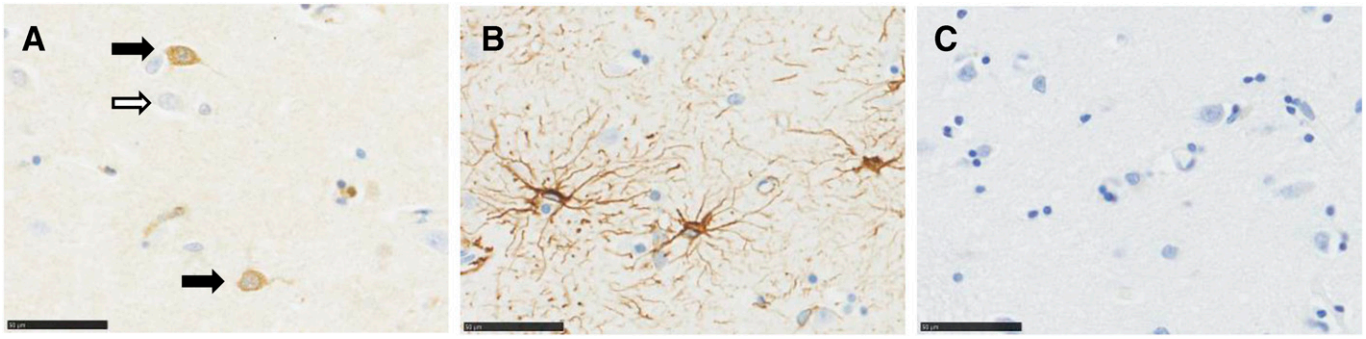

Fig. 7. GPR6 and GFAP expression in normal caudate putamen (female, 42 years old, nondemented control, neuropathologically normal). (A) GPR6 expression in putamen was analyzed using immunohistochemistry with H&E counterstain. GPR6 was expressed in a subpopulation of medium spiny neurons (GPR6-positive MSNs = filled arrow, GPR6-negative MSNs = empty arrow). (B) Assay positive control: GFAP was prominently expressed in astrocytes, using immunohistochemistry with H&E counterstain. (C) Negative control: negligible staining with rabbit immunoglobulin negative control, using immunohistochemistry with H&E counterstain. Scale bar, 50 μm.

efficacy. We have not specifically measured the impact of CVN424 on other signaling pathways but have observed that structurally related compounds were capable of comparably modulating both GPR6-cAMP and GPR6–β-arrestin assay systems (unpublished data). Thus, we cannot rule out that alternative signaling pathways may be contributing to the GPR6-mediated efficacy seen here.

As the intended therapeutic is for a CNS indication, it is important to demonstrate target occupancy in the brain and ultimately be able to correlate this to efficacy. To achieve this, we studied the binding of CVN424 in a receptor occupancy assay in both mice and rats and correlated these values with plasma concentrations. CVN424 achieved near maximal (i.e., >95%) receptor occupancy in both species, indicating good brain penetration and occupancy of the target. Although the absolute doses used across the two species to achieve ED_{50} differed (i.e., 0.34 and 7.25 mg/kg in mice and rats, respectively), the exposures required to achieve RO_{50} were equivalent (i.e., 6 and 7.4 ng/ml plasma concentration, respectively). Species-appropriate dose ranges were thus used for subsequent in vivo efficacy assessment.

The D1-type and D2-type MSNs of the direct and indirect pathways are morphologically indistinguishable but functionally distinct (Lenz and Lobo, 2013). They form two opposing circuits: the D1-expressing direct (striatonigral) pathway, which initiates motor activity, and the D2-expressing indirect (striatopallidal) pathway suppresses or terminates motor activity (Freeze et al., 2013). GPR6 is expressed in the indirect, D2-expressing MSNs, wherein its potential constitutive agonist activity is expected to increase levels of cAMP and activate the indirect pathway, which in turn decreases motor activity. In this study, we observe that CVN424, an inverse agonist against GPR6, increases locomotor activity. This is consistent with previous studies showing that GPR6 knockout mice have lower levels of cAMP and reduced adenylate cyclase activity in the striatum and display increased locomotor activity (Lobo et al., 2007; Oeckl et al., 2014). Additionally, we show that CVN424 reverses haloperidol-induced catalepsy. Haloperidol is a dopamine D2-receptor antagonist that produces catalepsy by elevating cAMP in the indirect pathway of the striatum (Kaneko et al., 1992). We propose that the ability for CVN424 to reverse catalepsy is likely a consequence of inverse agonism of the Gs-coupled GPR6 receptor counterbalancing the changes in cAMP induced by the Gi-coupled D2 receptor (Tanaka et al., 2007).

Parkinson disease is characterized by the loss of nigrostriatal dopaminergic neurons, which leads to motor deficits. In the current study, we investigated whether CVN424 could restore locomotor activity in rats that had the dopaminergic terminals depleted by bilateral injection of 6-OHDA into the striatum, a commonly used model for PD. This treatment resulted in an expected deficit in locomotor activity that could dose-dependently be fully reversed by CVN424 at a dose that equated to 72% GPR6 RO in the striatum. Furthermore, a previous study demonstrated that GPR6−/− mice had a reduced abnormal involuntary movements score in 6-OHDA unilaterally treated mice, indicating that GPR6 signaling is integral to the development of abnormal involuntary movements (Oeckl et al., 2014). Although this study investigated the effects of genetically depleting GPR6 signaling, it broadly supports our study and the utility of GPR6 as a beneficial treatment of motor dysfunction in Parkinson disease. This shows that CVN424, an inverse agonism of GPR6, is a promising approach for symptomatic treatment of Parkinson disease.

An important consideration when developing a therapeutic for a degenerative disease, such as PD, is to confirm that the intended target is present in the patient population and remains present as the disease progresses. Therefore, we investigated the expression of GPR6 in a cell type–specific manner from post-mortem samples from patients with Parkinson and compared this with nondemented controls. Similar to studies investigating the expression of GPR6 in rodents (Lobo et al., 2007), GPR6 in humans is preferentially expressed in the D2 receptor–expressing indirect pathway MSNs compared with direct D1 receptor–expressing MSNs, indicating that it may have a similar role in humans, as has been observed in rodents. Furthermore, we observed no change in GPR6 expression with disease despite the loss of primary input from the dopaminergic neurons. By investigating expression in a cell type–specific manner, we were able to determine that GPR6 message and protein are maintained in disease and selectively expressed within the indirect MSNs of the striatum.

In summary, we have demonstrated that CVN424 is a potent and selective inverse agonist for GPR6, an orphan GPCR that has enriched expression in the D2 receptor expressing (indirect) MSNs of the in the striatopallidal pathways within the striatum of both humans and rodents. In vivo, CVN424 increases locomotor activity when dosed alone and reverses haloperidol-induced catalepsy. Furthermore, CVN424 monotherapy produced a measurable reversal of the locomotor deficits induced by 6-OHDA striatal lesion, a common preclinical model for Parkinson disease. Taken together, these data indicate that an inverse agonist of GPR6, such as CVN424, has therapeutic potential for treating the motor symptoms of PD with a reduced risk of side effects, such as L-DOPA–induced dyskinesias. In this regard, CVN424 is currently being tested in a phase 2 study investigating its safety and efficacy in patients with Parkinson disease (ClinicalTrials.gov Identifier: NCT04191577).

Acknowledgments

We are grateful to Dr. D. Margolin for input and review of the manuscript; D. Cadwalladr for technical support for the NETSseq experiments; and Evan Nunez, Andreina Dyer, and Paul Rolzin for technical support for locomotor activity and haloperidol-induced catalepsy experiments.

Authorship Contributions

Participated in research design: Brice, Schiffer, Monenschein, Powell, Xu, Sheardown, Hosea, Hitchcock, Carlton.

Conducted experiments: Brice, Schiffer, Mulligan, Page, Cheung, Dickson, Kaushal, Lawrence, Sheardown, Chen, Bartkowski, Kanta, Russo.

Contributed new reagents or analytic tools: Monenschein, Sun, Murphy.

Performed data analysis: Brice, Schiffer, Mulligan, Page, Powell, Xu, Burley, Kaushal, Hosea.

Wrote or contributed to the writing of the manuscript: Brice, Schiffer, Mulligan, Powell, Xu, Cheung, Dawson.

References

Anders S, Pyl PT, and Huber W (2015) HTSeq–a Python framework to work with high-throughput sequencing data. *Bioinformatics* **31**:166–169.

Bellucci A, Mercuri NB, Venneri A, Faustini G, Longhena F, Pizzi M, Missale C, and Spano P (2016) Parkinson's disease: from synaptic loss to connectome dysfunction. *Neuropathol Appl Neurobiol* **42**:77–94

Breivogel CS, McPartland JM, and Parekh B (2018) Investigation of non-CB_1, non-CB_2 WIN55212-2-sensitive G-protein-coupled receptors in the brains of mammals, birds, and amphibians. *J Recept Signal Transduct Res* **38**:316–326.
Brooks DJ (2008) Optimizing levodopa therapy for Parkinson's disease with levodopa/carbidopa/entacapone: implications from a clinical and patient perspective. *Neuropsychiatr Dis Treat* **4**:39–47.
Chen JJ (2011) Pharmacologic safety concerns in Parkinson's disease: facts and insights. *Int J Neurosci* **121** (Suppl 2):45–52.
Cheng Y and Prusoff WH (1973) Relationship between the inhibition constant (K1) and the concentration of inhibitor which causes 50 per cent inhibition (I50) of an enzymatic reaction. *Biochem Pharmacol* **22**:3099–3108.
de Bie RMA, Clarke CE, Espay AJ, Fox SH, and Lang AE (2020) Initiation of pharmacological therapy in Parkinson's disease: when, why, and how. *Lancet Neurol* **19**: 452–461.
Dobin A, Davis CA, Schlesinger F, Drenkow J, Zaleski C, Jha S, Batut P, Chaisson M, and Gingeras TR (2013) STAR: ultrafast universal RNA-seq aligner. *Bioinformatics* **29**:15–21.
Dorsey ER and Bloem BR (2018) The Parkinson pandemic-A call to action. *JAMA Neurol* **75**:9–10.
Faraday MM (2002) Rat sex and strain differences in responses to stress. *Physiol Behav* **75**:507–522.
Freeze BS, Kravitz AV, Hammack N, Berke JD, and Kreitzer AC (2013) Control of basal ganglia output by direct and indirect pathway projection neurons. *J Neurosci* **33**:18531–18539.
Giorgi M, Melchiorri G, Nuccetelli V, D'Angelo V, Martorana A, Sorge R, Castelli V, Bernardi G, and Sancesario G (2011) PDE10A and PDE10A-dependent cAMP catabolism are dysregulated oppositely in striatum and nucleus accumbens after lesion of midbrain dopamine neurons in rat: a key step in parkinsonism physiopathology. *Neurobiol Dis* **43**:293–303.
Grabiec U and Dehghani F (2017) *N*-arachidonoyl dopamine: a novel endocannabinoid and endovanilloid with widespread physiological and pharmacological activities. *Cannabis Cannabinoid Res* **2**:183–196.
Hauser RA, Ellenbogen A, Khanna S, Gupta S, and Modi NB (2018) Onset and duration of effect of extended-release carbidopa-levodopa in advanced Parkinson's disease. *Neuropsychiatr Dis Treat* **14**:839–845.
Heiman M, Schaefer A, Gong S, Peterson JD, Day M, Ramsey KE, Suárez-Fariñas M, Schwarz C, Stephan DA, Surmeier DJ, et al. (2008) A translational profiling approach for the molecular characterization of CNS cell types. *Cell* **135**:738–748.
Ignatov A, Lintzel J, Kreienkamp H-JJ, and Schaller HC (2003) Sphingosine-1-phosphate is a high-affinity ligand for the G protein-coupled receptor GPR6 from mouse and induces intracellular Ca2+ release by activating the sphingosine-kinase pathway. *Biochem Biophys Res Commun* **311**:329–336.
Jenkins O, Bailey R, Crisp E, and Jackson DM (1980) Subacute L-DOPA in mice: biochemical and behavioural effects. *Psychopharmacology (Berl)* **68**:77–83.
Ji D, Jang CG, and Lee S (2014) A sensitive and accurate quantitative method to determine N-arachidonoyldopamine and N-oleoyldopamine in the mouse striatum using column-switching LC-MS-MS: use of a surrogate matrix to quantify endogenous compounds. *Anal Bioanal Chem* **406**:4491–4499.
Kaneko M, Sato K, Horikoshi R, Yaginuma M, Yaginuma N, Shiragata M, and Kumashiro H (1992) Effect of haloperidol on cyclic AMP and inositol trisphosphate in rat striatum in vivo. *Prostaglandins Leukot Essent Fatty Acids* **46**:53–57.
Kravitz AV, Freeze BS, Parker PRL, Kay K, Thwin MT, Deisseroth K, and Kreitzer AC (2010) Regulation of parkinsonian motor behaviours by optogenetic control of basal ganglia circuitry. *Nature* **466**:622–626.
Kriaucionis S and Heintz N (2009) The nuclear DNA base 5-hydroxymethylcytosine is present in Purkinje neurons and the brain. *Science* **324**:929–930.
Laun AS, Shrader SH, and Song ZH (2018) Novel inverse agonists for the orphan G protein-coupled receptor 6. *Heliyon* **4**:e00933.
Laun AS and Song Z-H (2017) GPR3 and GPR6, novel molecular targets for cannabidiol. *Biochem Biophys Res Commun* **490**:17–21.
Lenz JD and Lobo MK (2013) Optogenetic insights into striatal function and behavior. *Behav Brain Res* **255**:44–54.
Lobo MK, Cui Y, Ostlund SB, Balleine BW, and Yang XW (2007) Genetic control of instrumental conditioning by striatopallidal neuron-specific S1P receptor Gpr6. *Nat Neurosci* **10**:1395–1397.
Mansouri A, Taslimi S, Badhiwala JH, Witiw CD, Nassiri F, Odekerken VJJ, De Bie RMA, Kalia SK, Hodaie M, Munhoz RP, et al. (2018) Deep brain stimulation for Parkinson's disease: meta-analysis of results of randomized trials at varying lengths of follow-up. *J Neurosurg* **128**:1199–1213.
Martin M (2011) Cutadapt removes adapter sequences from high-throughput sequencing reads. EMBnet j **17**:10
Müller T (2017) Current and investigational non-dopaminergic agents for management of motor symptoms (including motor complications) in Parkinson's disease. *Expert Opin Pharmacother* **18**:1457–1465.
Nutt JG and Bohnen NI (2018) Non-dopaminergic therapies. *J Parkinsons Dis* **8** (Suppl 1):S73–S78.
Oeckl P and Ferger B (2016) Increased susceptibility of G-protein coupled receptor 6 deficient mice to MPTP neurotoxicity. *Neuroscience* **337**:218–223.
Oeckl P, Hengerer B, and Ferger B (2014) G-protein coupled receptor 6 deficiency alters striatal dopamine and cAMP concentrations and reduces dyskinesia in a mouse model of Parkinson's disease. *Exp Neurol* **257**:1–9.
Paxinos G and Watson C (2007) *The Rat Brain in Stereotoxic Coordinates*, 6th ed Elsevier Inc., Amsterdam.
Poewe W and Mahlknecht P (2020) Pharmacologic treatment of motor symptoms associated with Parkinson disease. *Neurol Clin* **38**:255–267.
Pollak P (2013) *Deep Brain Stimulation for Parkinson's Disease - Patient Selection*, 1st ed, Elsevier B.V., Netherlands.
Robles JA, Qureshi SE, Stephen SJ, Wilson SR, Burden CJ, and Taylor JM (2012) Efficient experimental design and analysis strategies for the detection of differential expression using RNA-Sequencing. *BMC Genomics* **13**:484.
Ryan MB, Bair-Marshall C, and Nelson AB (2018) Aberrant striatal activity in parkinsonism and levodopa-induced dyskinesia. *Cell Rep* **23**:3438–3446.e5.
Salat D and Tolosa E (2013) Levodopa in the treatment of Parkinson's disease: current status and new developments. *J Parkinsons Dis* **3**:255–269.
Shrader SH and Song ZH (2020) Discovery of endogenous inverse agonists for G protein-coupled receptor 6. *Biochem Biophys Res Commun* **522**:1041–1045.
Strange PG (2008) Agonist binding, agonist affinity and agonist efficacy at G protein-coupled receptors. *Br J Pharmacol* **153**:1353–1363.
Tanaka S, Ishii K, Kasai K, Yoon SO, and Saeki Y (2007) Neural expression of G protein-coupled receptors GPR3, GPR6, and GPR12 up-regulates cyclic AMP levels and promotes neurite outgrowth. *J Biol Chem* **282**:10506–10515.
Uhlenbrock K, Gassenhuber H, and Kostenis E (2002) Sphingosine 1-phosphate is a ligand of the human gpr3, gpr6 and gpr12 family of constitutively active G protein-coupled receptors. *Cell Signal* **14**:941–953.
Wang L, Wang S, and Li W (2012) RSeQC: quality control of RNA-seq experiments. *Bioinformatics* **28**:2184–2185.
Whitmer D, de Solages C, Hill B, Yu H, Henderson JM, and Bronte-Stewart H (2012) High frequency deep brain stimulation attenuates subthalamic and cortical rhythms in Parkinson's disease. *Front Hum Neurosci* **6**:155.
Xu X, Stoyanova EI, Lemiesz AE, Xing J, Mash DC, and Heintz N (2018) Species and cell-type properties of classically defined human and rodent neurons and glia. *eLife* **7**:1–47.
You H, Mariani L-L, Mangone G, Le Febvre de Nailly D, Charbonnier-Beaupel F, and Corvol J-C (2018) Molecular basis of dopamine replacement therapy and its side effects in Parkinson's disease. *Cell Tissue Res* **373**:111–135.

Address correspondence to: Nicola L. Brice, Cerevance Ltd., 418 Cambridge Science Park, Cambridge CB4 0PZ, UK. E-mail: Nicola.brice@cerevance.com